Vietnam Journal of Science and Technology ***60*** *(6) (2022) 1044-1055*

doi:10.15625/2525-2518/16473

BIOLOGICAL MACROFOULING AND ELECTROCHEMICAL CORROSION PROPERTIES OF STRUCTURAL STEEL AH36 IN NATURAL SEAWATER AT HON TRE ISLAND, NHA TRANG

Nguyen Van Chi[1, *], Dong Van Kien[1], Le Hong Quan[1], Cao Nhat Linh[1], Nong Quoc Quang[1], Nguyen Duc Anh[1], Pham Thi Hai Yen[2], Le Quoc Hung[2]

[1]*Coastal Branch, Vietnam-Russia Tropical Center, 30 Nguyen Thien Thuat, Nha Trang, Khanh Hoa, Viet Nam*

[2]*Institute of Chemistry, Vietnam Academy of Science and Technology, 18 Hoang Quoc Viet, Cau Giay, Ha Noi, Viet Nam*

[*]Email: *nguyenvanchirvtc@gmail.com*

Received: 23 August 2021; Accepted for publication: 12 November 2022

Abstract. The biological macrofouling characteristics and electrochemical corrosion behavior of structural steel AH36 in natural seawater were studied continuously for 12 months at Hon Tre Island, Nha Trang, Viet Nam. Electrochemical corrosion properties were studied using a PPGS-HHMC12 multi-channel device produced by the Institute of Chemistry, Vietnam Academy of Science and Technology. Tests were conducted at depths of 0.6 m, 1.8 m, and 3.0 m; under anti-macrofouling control, rotary movement, and under laboratory conditions as a comparison option. The results showed that macro-fouling formed and grew rapidly in both quantity, size and biomass in the next 3 months, then slowly and stably increased to about 8 months (6.06 $kg.m^{-2}$). The OCP shifted to a positive potential, then reached a stable value of about -550 mV during the rest of exposure time. The corrosion current density decreased sharply from the first month to the fourth month, then reached a stable value of about 10 $\mu A.cm^{-2}$ in next months of testing. The corrosion rate of AH36 steel in natural seawater in the field was higer than that under laboratory condition, which could be explained by the interaction of many factors such as dissolved oxygen, biofouling, water current, solar radiation.

Keywords: AH36 structural steel, bio-macrofouling, electrochemical corrosion, natural seawater, field test, rotary test.

Classification numbers: 2.9.1, 2.10.3, 3.1.2.

1. INTRODUCTION

Biological fouling is caused by the deposition and growth of organisms on surfaces of studied samples in seawater. Bacteria are the most likely to cause problems in standard stainless steel and many other materials, which are corroded by reducing sulfate to hydrogen sulfide [1]. Offshore structures, commercial ships, mooring lines, submersible pipelines, coastal wharves are mainly constructed from mild or low alloy structural steels [2]. Bio-fouling affects structural integrity, increases corrosion, and destroys metal fatigue [3]. They are very diverse, such as seaweed, coral, oysters, barnacles, mussels, etc., which directly affect corrosion during the

maturation process [4]. In some cases, however, the macrofouling population on the surface of the materials could create a barrier that prevented oxygen from contacting the substrate, thus leading to reduced corrosion [5].

Corrosion of steel in seawater is complicated, influenced by many factors and their interactions [6]. They could be divided into four groups of fundamental factors, namely: physical parameters, seawater chemical properties, biological fouling, and material characteristics [7]. Tribo-corrosion is a material deterioration or transformation resulting from simultaneous action of wear and corrosion in seawater [8, 9]. The simultaneous process of wear and corrosion is also known as destructive corrosion [8 - 10]. The difficulty in studying this corrosion phenomenon is that our understanding of abrasion and chemical corrosion is insufficient to predict aggregate corrosion behavior [9]. In the seawater environment, the relative motion between surfaces produced by waves, ocean currents leads to a process of continuous wear in the contacting surfaces; meanwhile, electrochemical corrosion still occurs as another considerable important phenomenon [11]. Variations in the chemistry of open ocean seawater tend to take place slowly over periods of a few to several months. Such gradual changes may produce an equally gradual change in the corrosion rate of structural materials with season and location. However, they are unlikely to produce sharp changes in either the corrosion mechanism or the corrosion rate [12].

In electrolyte solutions, electrochemical techniques provide on-site and real-time control of the surface reactivity of metals and other conductive materials. These techniques are widely used in corrosion science and are increasingly applied in corrosion experiments that help understand how wear and biofouling could affect corrosion kinetics [10]. Besides, the influence of chemical reactions on the mechanical behavior of the contact surfaces can also be evaluated [13]. From that, it opens the way to solve the problem of electrochemical corrosion in the natural seawater environment.

This study investigated biological macrofouling characteristics and electrochemical corrosion properties of structural steel AH36 in natural seawater at Hon Tre Island, Nha Trang, Viet Nam. In addition, testing in natural seawater at laboratory conditions with or without water movement was studied for comparison and additional evaluation.

2. MATERIALS AND METHODS

2.1. Materials, method, and devices

AH36 structural steel sheets were used as samples with the following compositions in wt%: C ≤ 0.18; Si ≤ 0.5; Mn ≤ 0.9; Cr ≤ 0.2; Cu ≤ 0.05; Ni ≤ 0.4; Mo ≤ 0.08; P ≤ 0.035; S ≤0.035; Nb ≤ 0.02; Ti ≤ 0.02; Al ≤ 0.015, and balance Fe.

AH36 steel samples with a 300 cm^2 working area were fabricated with dimensions of 10×15×0.4 cm, marked with numeric symbols, abraded with SiC polishing paper, cleaned from oil, grease, dirt, and corrosion product following ISO 8407, then stored in the desiccator before a test.

Electrochemical corrosion properties were studied using a PPGS-HHMC12 multi-channel device produced by the Institute of Chemistry, Vietnam Academy of Science and Technology. A three-electrode system was used with a stainless steel auxiliary electrode, an $Ag/AgCl_2$ reference electrode, and AH36 steel samples as the working electrode.

Seawater parameters were measured at the same location of testing specimens. The dissolved oxygen content measurement was carried out using a portable meter AM 40 (Meinberg, Germany). The pH and temperature were measured with an HI 8314 pH meter

(Hanna Instruments, Italia). Salinity was determined using an HI 98319 refractometer (Hanna Instruments, Italia).

With the dynamic test in the laboratory, the studied seawater slip flow over the sample surface with a velocity of 0.2 m/s was performed by a submersible pump AP5600 IPX8 (LifeTech, China). The flow velocity was measured by Global Water Flow Probe FP211 (Global Water Instrument, USA).

2.2. Study on bio-macrofouling characteristics on AH36 steel substrate

Samples were deployed in natural seawater (At Marine Experimental Research Station, Vietnam-Russia Tropical Center, Dam Bay coastal area, Hon Tre Island, Nha Trang Bay, Viet Nam) following ISO 11306 (F symbol group, here F stand for Field). Five different testing conditions were performed :

- At 3 depths of 0.6 m (F – 0.6 m), 1.8 m (F – 1.8 m), and 3 m (F – 3.0 m);

- In the rectangular box frame, covered by plastic net with a mesh size of 50 μm (or 300 mesh), to prevent macro fouling at a depth of 0.6 m (called anti-macrofouling sample, F - anti macro);

- On rotary movement rack at the same depth of 0.6 m (rotary sample, F - rotary).

Three tested samples of each condition were collected monthly. Fouling organisms were identified to genus and species level following previous records from the study regions [14 - 16].

After each testing period, the biomass formed on sample substrates was allowed to dry naturally in the air for some days. After that, they were dried in an oven at 100 °C to constant weight to an accuracy of 10^{-2} g [16]. The biomass was expressed as $kg.m^{-2}$.

2.3. Study on electrochemical corrosion properties of AH36 steel

For the electrochemical corrosion test, the AH36 steel sheets (dimensions of 5 × 7 × 0.4 cm, with 75 cm^2 working area) were prepared as item 2.1. One 2.5-core shielded cable was welded to samples to connect to the device when measuring. Samples were deployed in the same condition as the biofouling test.

In addition, samples were tested in natural seawater in two tanks, 1000 L each (Ø146-118 × 79 cm) at the laboratory under two different conditions (L symbol group): Without the flow (velocity = 0, static test, L - static) and with the flow (velocity of 0.2 m/s, dynamic test, L - flow), see item 2.1. Natural seawater was renewed every two months after measurement. Three test samples were performed for each study condition.

Open circuit potential was determined before linear polarization. The voltage was scanned between ± 100 mV vs. OCP with a scan rate of 1 mV/s. Corrosion parameters were determined using the Stern-Geary equation.

To determine the area of pitting corrosion on the sample's surface, after removing biological fouling and corrosion products, the area of pitting corrosion was identified (by ISO 11463), then marked by colored pencil. After that, ImageJ software was used to determine the pitting corrosion percentage.

3. RESULTS AND DISCUSSION

3.1. Some characteristic parameters of seawater at different testing conditions

As shown in Table 1, the environmental parameters of seawater at the Hon Tre Island and in the Lab were almost similar. The difference was found only in dissolved oxygen concentrations (DO). In the laboratory, especially in static condition (approx. 1.7 mg/L), DO is much lower than that on HonTre Island (approx. 7.5 mg/L). The low DO in static condition was due to the less oxygen absorption of oxygen from the air into the water and DO consume by oxidation reaction of Fe^{2+} formed by corrosion of studied samples in the tank. The flow of 0.2 m/s enables oxygen to dissolve into the water due to diffusion and convection [17], therefore DO increases significantly (approx. 6.7 mg/L).

Table 1. Some parameters of the seawater at Hon Tre islands, Nha Trang.

No.	Test site		Temperature (°C)	pH	Salinity (‰)	Dissolved oxygen (mg/L)
1	At Hon Tre Island	at a depth of 0.6 m	25.1 ÷ 30.3	8.04 ÷ 8.22	32 ÷ 35	7.51 ÷ 9.33
2		at a depth of 1.8 m	25.9 ÷ 29.1	8.03 ÷ 8.19	32 ÷ 35	7.52 ÷ 9.40
3		at a depth of 3.0 m	26.1 ÷ 29.6	8.01 ÷ 8.24	32 ÷ 35	7.43 ÷ 9.25
4	In the tank at Lab	without velocity	27.8 ÷ 30.3	7.76 ÷ 8.08	34 ÷ 35	1.72 ÷ 2.94
5		with velocity	28.1 ÷ 30.9	7.59 ÷ 7.99	34 ÷ 35	6.67 ÷ 7.54

3.2. Macro-fouling characteristics and biomass in natural seawater

3.2.1. Macro-fouling characteristics on the sample surface

The photos of the samples after different periods of 1, 3, 6, 9, 12 months of exposure at various conditions are shown in Figure 1. It was observed that the surface of the specimens was essentially the same in the first month of testing. Red yellow and black surfaces were typical for iron-based corrosion products. A microbial film had formed on the entire surface as well. However, if taken a closer look, some marine larvae (white spots) dotted the surface of the test samples at three different depths (Fig. $1_{a\text{-}c,e}$). The number of spots was less on the rotary test specimen (Fig. 1_e) and were not found on the macro antifouling test specimen (Fig. 1_d).

The fouling development on the AH36 sample's surface after exposure of 3, 6, 9, 12 months at various conditions are shown in Fig. 1. Fouling at the three natural testing depths was composed of various organisms such as algae, barnacles, bryozoans, polychaete worms, compound and straightforward ascidians, and oysters (Fig. $1_{a\text{-}c}$).

The Bio-macrofouling had covered almost the entire surface after three months. The growth of the biofouling species by the 6th month had spread beyond the sample edge and continued after that. As observed on the sample surface during exposure, the fouling development at the three depths was almost the same. This result could be explained because the environmental conditions at these three depths were relatively similar. It could be seen that the fouling developed on the rotary samples more slowly and much less than that of the other samples (Fig. 1_e). It can be explained that the rotary movement of the sample in seawater limited the contacting and nesting of the larvae. The main factor determining the tendency of a surface to foul when exposed to the sea may be the number of larvae coming into contact with the exposed surface [17].

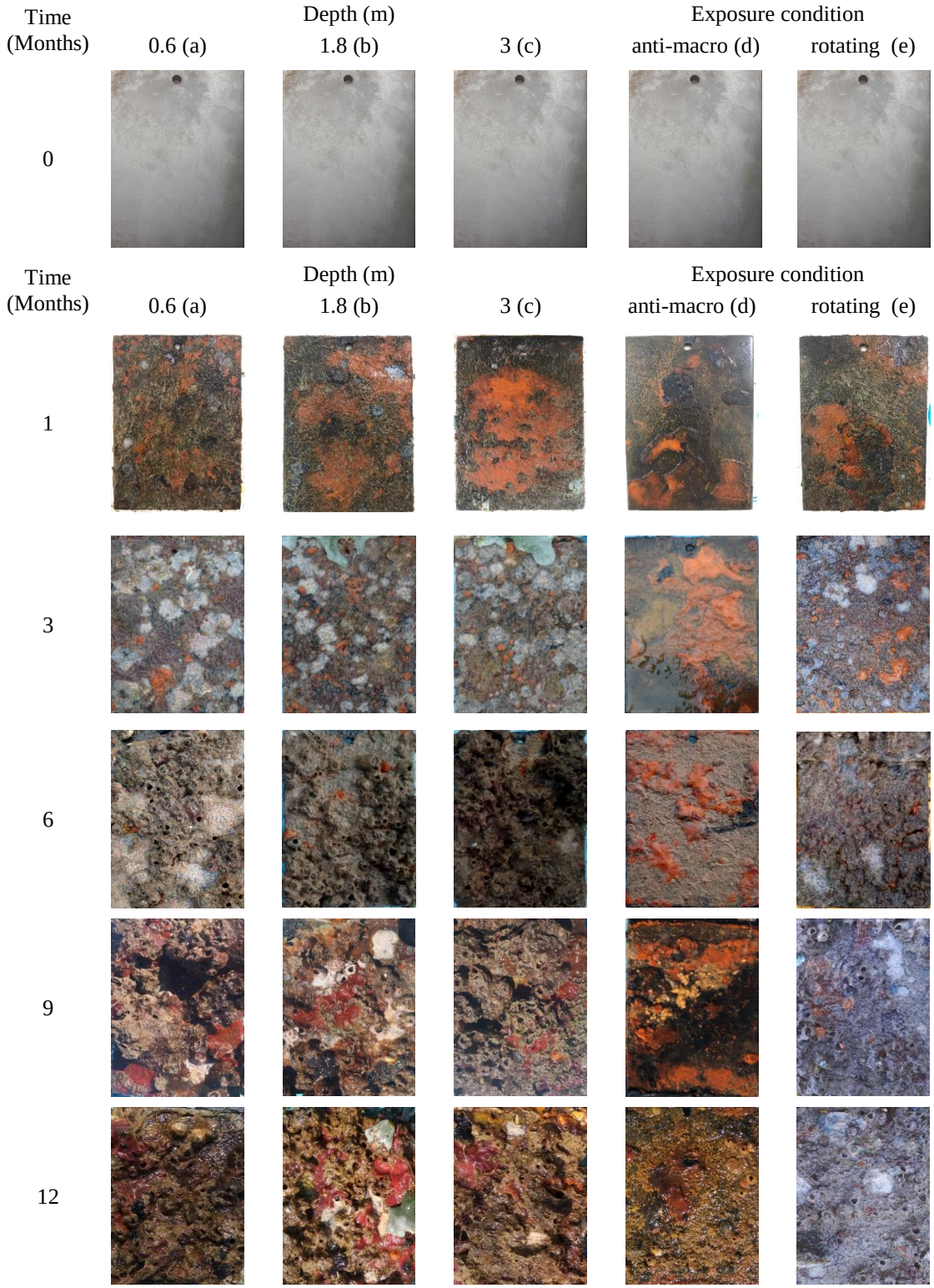

Figure 1. Images of fouling development on the sample surface.

Attachment and growth of barnacles on sample surface also depend on the rotational speed of the sample, and fouling was inversely proportional to the rotational speed [18]. Fig. 1_d also showed that no macrofouling was found on the surface of the anti-macrofouling sample. Thus, it could be seen that the mesh size is small enough to prevent larvae from contacting the sample. Even so, there were a few barnacles but not significant on the test sample after twelve months.

3.2.2. Biomass on the sample surface

Figure 1 showed that the biomass in the first month of all studied samples was almost negligible. Negligible biomass was also obtained in the case of a macro-antifouling sample during 12 months. The biomass on the sample surfaces at three different testing depths and the rotary sample were depicted in Figure 2.

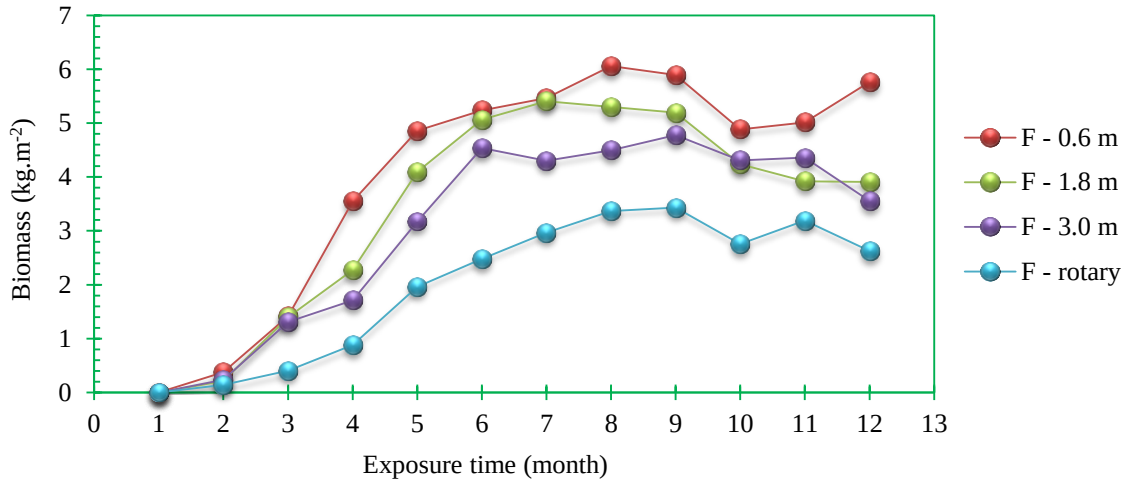

Figure 2. The biomass load on structural steel substrate AH36 monthly at different conditions.

In the first two months, the biomass was relatively small and then increased much faster in the period from the third to the seventh month. This result showed that the fouling species had grown enormously in quantity, size, and weight. The biomass increase slowed down and changed unstable after the ninth month. The biomass on the rotary test sample was also smaller than the rest of the samples during the whole test. This result was consistent with the observation shown in Fig. 1. It also showed that the rotary movement of specimens restricted the contact ability of the larvae to the surface and limited their growth when they were nested on the surface. Figure 2 showed that the biomass of the samples at depths of 0.6 m and 1.8 m was slightly higher than that of the sample at 3.0 m in a period of steady growth. This result was able to be explained by the more potent phototrophic phenomenon of the surface water layer.

3.3. AH36 structural steel corrosion properties in natural seawater

3.3.1. Trend of OCP

The open-circuit potential variation can reflect the surface state of the material in solution. Therefore analysis of this value during the test allows more detailed information of corrosion process on the sample surface [19]. The variation of OCP of AH36 structural steel samples immersed in seawater over time was presented in Figure 3.

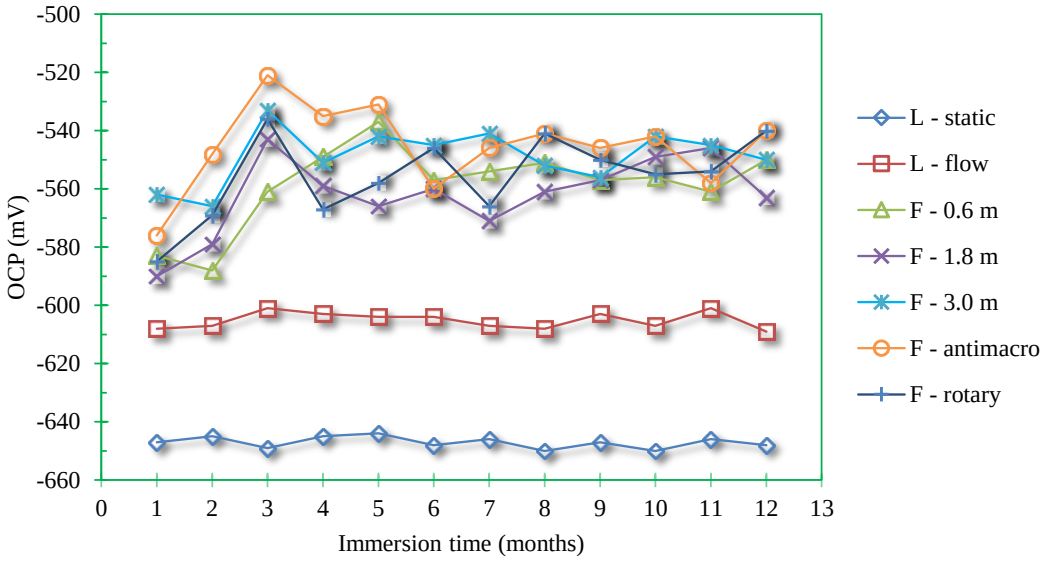

Figure 3. Variation of OCP with testing time.

It could be seen that OCP values of samples in the laboratory (L-static and L-flow) were almost unchanged but distinctly different. In the condition of flow, the OCP value of structural steel sample AH36 shifted to the positive potential about 40 mV. As known, agitated aqueous media produces higher dissolved oxygen concentrations [20]. This condition also created more oxygen vacancies on the surface [21]. Corrosion mechanism in the presence of gas always produces multilayer corrosion products, which tend to be rich in the metal inside and rich in oxygen outside [22]. A higher concentration of dissolved oxygen accelerates the cathodic process. As a result, the OCP shifted to a positive value, as it would trigger a faster dissolution of the metal in the electrolyte solution. Meanwhile, the continuous sliding of the water stream would disrupt the layer of corrosion products that had formed temporarily on the surface of the sample. In a stable physicochemical environment, the combination of these two factors led to the sample's surface always being in a more active state.

In natural seawater, on studied sites (F symbol group), it was observed that the OCP of steel electrode was moved toward more positive values during the first three months of immersion, then relatively stable with immersion time. During the first 3 months of testing, the sample was exposed to seawater for almost the entire surface. Higher concentrations of dissolved oxygen, vibration of the sample due to waves, and ocean currents would trigger a higher degree of corrosion of the steel. In addition, this was also the stage of forming the most complete microbial population on the sample surface. As mentioned in Section 3.2.1, from the 3rd month onwards, macro-fouling started to form and spread over the entire sample surface.

3.3.2. Electrochemical corrosion parameters

Figure 4 shows the polarization curves of the AH 36 steel after 1 and 6 months of immersion in seawater. Visually, it could be roughly estimated that the steeper polarization curve, the higer corrosion rate. Thus, in the first month of testing (Figure 3), the corrosion rate of the samples tested in natural seawater in the field was much higher than that of the samples tested in the laboratory. At the same time, in the laboratory, the test specimen with the flow also

had a higher corrosion rate. This difference in slope (or corrosion rate) decreased after 6 months of testing.

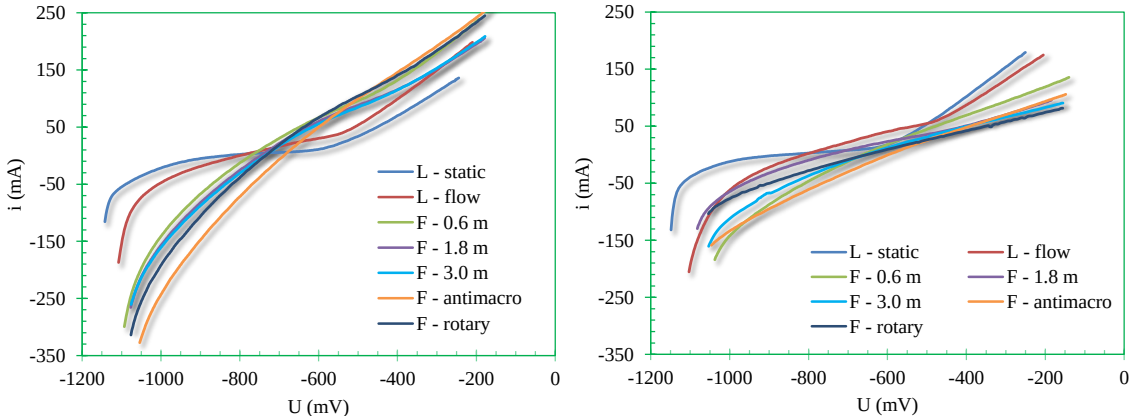

Figure 4. Polarization curves of AH36 steel under different conditions after one and six months of test.

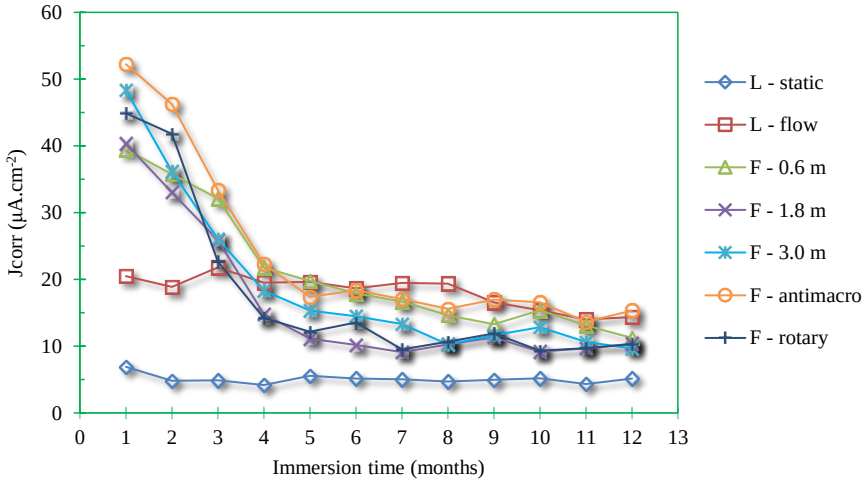

Figure 5. Corrosion current density of AH36 steel under different conditions by immersion time.

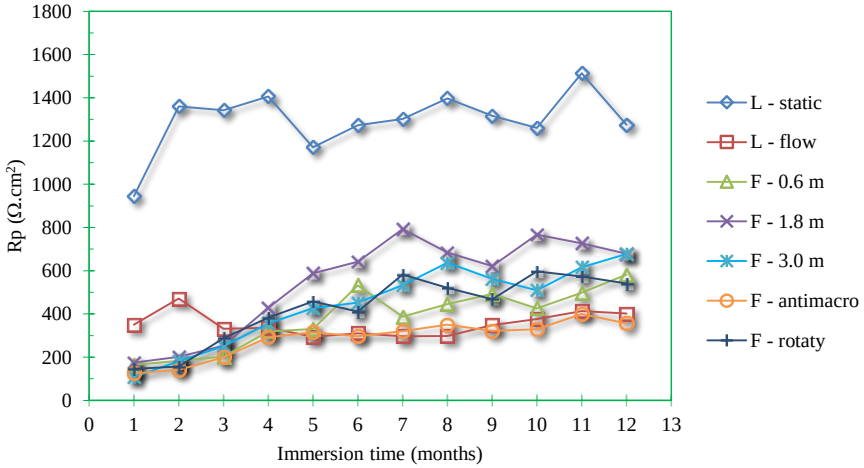

Figure 6. Polarization resistance of AH36 steel under different conditions by immersion time.

The variation of the calculated electrochemical corrosion parameters versus immersion time was presented in Figures 5, 6. It could be seen that the corrosion current density or polarization resistance of the sample in seawater at the laboratory conditions was relatively stable. This result is consistent with the trend of variation in OCP value as discussed above. The corrosion current density of the static sample reached a steady value of around 5 $\mu A.cm^{-2}$ throughout the entire test period. This means that the corrosion rate was quite stable. In the case of the water slide sample, the corrosion current density was 4-fold higher, compared with those of the static sample in the first eight months, and was about 3-fold higher in the last four months. It was known that the layer of corrosion products formed on the metal substrate always played as a barrier to limit the dissolution of metal ions into the electrolyte solution and oxygen in contact with the metal surface. As mentioned in Section 3.3.1, contrary to the static sample, when the sample contacts with water flow at a higher dissolved oxygen concentration and limitation of the formation corrosion-product layer by wear certainly increased the corrosion rate.

In the natural marine environment at Hon Tre Island, the initial corrosion current density was much higher than that in the seawater in laboratory condition (8-10-fold compared to that of the static test and 2-3-fold compared to that of the dynamic test). This result proved that the actual corrosion of AH36 steel in natural seawater was much more robust, especially of the anti-macrofouling sample. It could be explained by the combined and synergistic effects of many factors in seawater. However, the magnitude of the current density decreased rapidly until the fourth month or fifth month of testing duration. This result was associated with a contact time, nesting of biofouling on the entire surface, as shown in Figures 1 and 2. The strong form of the macrofouling population after the third month significantly limited the corrosion rate of AH36 steel in seawater. With the anti-macrofouling sample, although there was almost no macro fouling developed on the surface during the study period, the constitution of the corrosion products layer also helped to hinder the further corrosion at a later stage.

3.3.3. Surface corrosion characteristics of samples with biofouling

Figure 7 showed photos of samples after 12 months of testing under different conditions that were removed from all biological fouling and corrosion products. It could be seen that the static test specimen surface was relatively smooth as a result of uniform corrosion, while the water slid test specimen was rough. This phenomenon could be explained by the mechanical effect of water flow combined with the acceleration of corrosion by high dissolved oxygen concentration, causing the ununiform corrosion of that sample. The appearance of pitting spots on the surface of samples at different depths and rotary samples indicated the formation of pitting corrosion caused by biological macrofouling. On the other hand, the surface morphology of the anti-macrofouling sample was rough and patchy, which was consistent with the highest corrosion current density of this sample. Thus, it could be commented that, in the case of only limiting the formation of macro-fouling, the microbiological corrosion process still occurs unevenly on the entire surface. Meanwhile, the pitting corrosion could be caused by a few biofouling individuals corroding deeper into the sample. The size, shape, and depth of the corrosion pits on testing specimen surfaces also varied irregularly during the entire test. This phenomenon could be explained by the random attachment and nesting of marine organisms in the sample.

The variability of the spot corrosion area of the field test specimens over time is shown in Figure 8. There was an increase in the corrosion area during the six months of testing. This can be explained by the growth period of marine fouling. However, there was no significant difference in spot corrosion area between the test conditions.

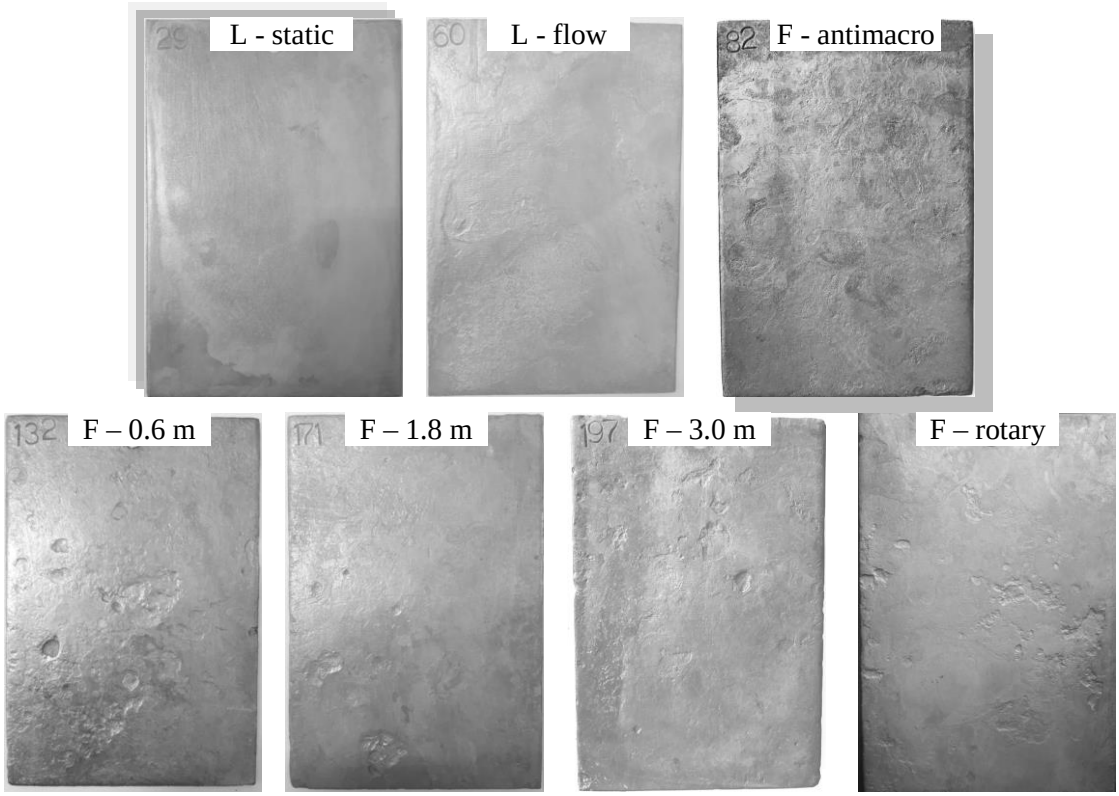

Figure 7. Sample surface morphology after 12 months of testing

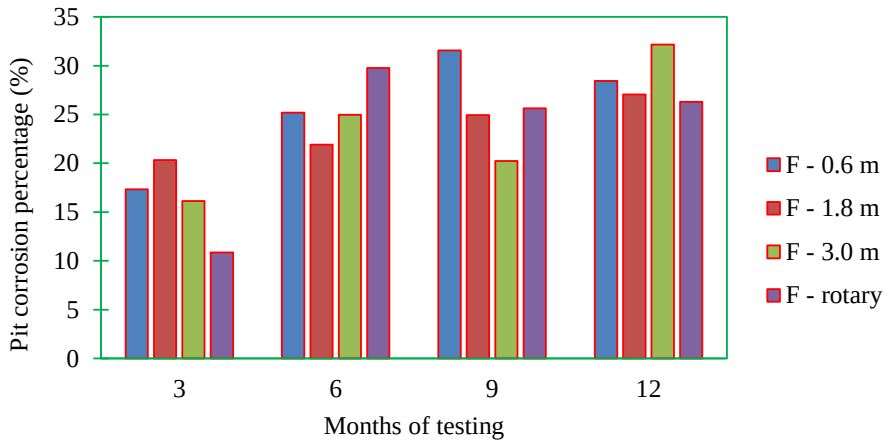

Figure 8. Percentage of pit corrosion area on sample surface during 12 months of testing.

4. CONCLUSIONS

- Biological fouling formed on the surface of AH36 structural steel as a microbial film during the first month of exposure, followed by macro-fouling populations. Macro-fouling formed and grew rapidly in both quantity, size and biomass in the next 3 months, then slowly and stably increased to about 8 months.

- Based on electrochemical parameters, corrosion rate of structural steel AH36 in seawater was affected by the interaction of many factors such as dissolved oxygen, biofouling, water current, solar radiation. Corrosion proccess occurred rapidly in the first two months of testing, then decreased and stabilized at about 10 $\mu A.cm^{-2}$ after four months. In case of anti-macrofouling or rotary movement, the corrosion rate of the steel was higher because it is not or less affected by macro-fouling. The primary forms were uniform and pitting corrosion caused by the combination of tribo-corrosion and biological fouling. The corrosion rate of AH36 steel in natural seawater in the field was many times higher than in laboratory conditions.

Acknowledgments. This section is devotes to acknowledging the supports by the research funding from Vietnam - Russia Tropical Center.

CRediT authorship contribution statement. Nguyen Van Chi: Supervision, Methodology, Formal analysis, Investigation, Conceptualization, Manuscript writing, Editing. Dong Van Kien, Le Hong Quan, Cao Nhat Linh, Nong Quoc Quang, Nguyen Duc Anh: Experiment, Formal analysis, Investigation, Software. Pham Thi Hai Yen, Le Quoc Hung: Electrochemical measurement equipment setup, Methodology, Data analysis.

Declaration of competing interest. The authors declare that they have no known competing financial interests or personal relationships that could have influenced the work reported in this paper.

REFERENCES

1. Hesselgreaves J. E., Law R., and Reay D. A. - Compact Heat Exchangers in Practice, in Compact Heat Exchangers, Charter 8, 2nd ed. (2017), Elsevier Ltd., 2017, pp. 361-400. https://doi.org/10.1016/b978-0-08-100305-3.00008-2.
2. Melchers R. E. - Principles of Marine Corrosion, Charter 6, in Springer Handbook o*f* Ocean Engineering, Springer, 2016, pp. 111-126.
3. Thomas C. J., Edyvean R. G. J., and Brook R. - Biologically enhanced corrosion fatigue, Biofouling **1** (1) (1988) 65-77. https://doi.org/10.1080/08927018809378096.
4. Lewis J. R. and Mercer A. D. - Corrosion and marine growth on offshore structures, United States, 1984.
5. Ting O. S., Potty N. S., and Liew M. S. - Prediction of corrosion rates in marine and offshore structures, 2011 National Postgraduate Conference - Energy and Sustainability: Exploring the Innovative Minds, NPC 2011 (2011) 1-6. https://doi.org/10.1109/ NatPC.2011.6136376.
6. Melchers R. E., Moan T., and Gao Z. - Corrosion of working chains continuously immersed in seawater, Journal of Marine Science and Technology **12** (2) (2007) 102-110. https://doi.org/10.1007/s00773-006-0227-4.
7. Bhandari J., Khan F., Abbassi R., Garaniya V., and Ojeda R. - Modelling of pitting corrosion in marine and offshore steel structures - A technical review, Journal of Loss Prevention in the Process Industries **37** (2015) 39-62. https://doi.org/10.1016/ j.jlp.2015.06.008.
8. Celis J. P. and Ponthiaux P. - Testing tribocorrosion of passivating materials supporting research and industrial innovation, Handbook. Maney publishing, 2012. ISBN: 978-1-907975-20-2.
9. Mischler S. - Triboelectrochemical techniques and interpretation methods in

tribocorrosion: A comparative evaluation, Tribology International **41** (7) (2008) 573-583. https://doi.org/10.1016/j.triboint.2007.11.003.

10. Landolt D., Mischler S., and Stemp M. - Electrochemical methods in tribocorrosion: A critical appraisal, Electrochimica Acta **46** (24 - 25) (2001) 3913-3929. https://doi.org/10.1016/S0013-4686(01)00679-X.
11. Vázquez-Hernández A. O., Ellwanger G. B., and Sagrilo L. V. S. - Long-term response analysis of FPSO mooring systems, Applied Ocean Research **33** (4) (2011) 375-383. https://doi.org/10.1016/j.apor.2011.05.003.
12. Zayed W. G. A., Guedes Soares C., Garbatov Y. - Environmental factors affecting the time dependant corrosion wastage of marine structures, in Proceedings of 11th International Congress of the International Maritime Association of the Mediterranean, 2005, pp. 589-598.
13. Landolt D. - Electrochemical and materials aspects of tribocorrosion systems, Journal of Physics D: Applied Physics **39** (15) (2006) 3121-3127. https://doi.org/10.1088/0022-3727/39/15/S01.
14. Maruthamuthu S., Eashwar M., Manickam S. T., Ambalavanan S., Venkatachari G., and Balakrishnan K. - Marine fouling on test panels and in-service structural steel in Tuticorin harbour, Indian Journal of Geo-Marine Sciences **19** (1) (1990) 68-70. http://nopr.niscair.res.in/handle/123456789/38199
15. Eashwar M., Maruthamuthu S., and Manickam S. T. - An assessment of preference for coupon positions by tropical marine fouling organisms, Biofouling **3** (4) (1991) 277-286. https://doi.org/10.1080/08927019109378182.
16. Palanichamy S., Subramanian G., and Eashwar M. - Corrosion behaviour and biofouling characteristics of structural steel in the coastal waters of the Gulf of Mannar (Bay of Bengal), India, Biofouling **28** (5) (2012) 441-451. https://doi.org/10.1080/08927014.2012.684947.
17. WHOI (Woods Hole Oceanographic Institute) - Factors Influencing the Attachment and Adherence of Fouling Organisms, in Marine Fouling and Its Prevention, Charter 13 (580) (1952), George Banta Publishing Co., 1952, pp. 230-240.
18. Smith F. G. W. - Effect of water currents upon the attachment and growth of barnacles, The Biological Bulletin **90** (1) (1946) 51-70. https://doi.org/10.2307/1538061.
19. Celis J. P., Ponthiaux P., and Wenger F. - Tribo-corrosion of materials: Interplay between chemical, electrochemical, and mechanical reactivity of surfaces, Wear **261** (9) (2006) 939-946. https://doi.org/10.1016/j.wear.2006.03.027.
20. https://www.sierraclub.org/sites/www.sierraclub.org/files/sce/river-prairie-group/WaterProject/InternalDocumentation/do1.pdf, RPG River Monitoring Program 2003, (accessed 23 August 2021).
21. Feng Z., Cheng X., Dong C., Xu L., and Li X. - Effects of dissolved oxygen on electrochemical and semiconductor properties of 316L stainless steel, Journal of Nuclear Materials **407** (3) (2010) 171-177. https://doi.org/10.1016/j.jnucmat.2010.10.010.
22. Danielewski M. - Gaseous Corrosion Mechanisms, in Corrosion: Fundamentals, Testing, and Protection, ASM Handbook, ASM International **13A** (2003) 106-114. https://doi.org/10.31399/asm.tb.cpi2.t55030062.